RSC Advances

ROYAL SOCIETY OF CHEMISTRY

www.rsc.org/advances

Journal Name

RSCPublishing

ARTICLE

S_4N_4 as an intermediate in Ag_2S nanoparticles synthesis

Cite this: DOI: 10.1039/x0xx00000x

Baskaran Ganesh Kumar and Krishnamurthi Muralidharan*

Received ooth January 2012,
Accepted ooth January 2012

DOI: 10.1039/x0xx00000x

www.rsc.org/

Hexamethyldisilazane assisted synthesis of Ag_2S nanoparticles is demonstrated. Classical chemical investigations and nano investigations were utilized to explain the formation of nanoparticles. Controlled reactions were performed to explain the reaction mechanism. While establishing the reaction mechanism, Ag nanoparticles and tetrasulfur tetranitride (S_4N_4) formation was identified. Controlled reaction explained that the sulfur reduction occurred through S-N polymeric intermediate. Then the polymeric intermediate decomposed to tetrasulfur tetranitride. Formation of S_4N_4 was unambiguously confirmed by the single crystal X-ray diffraction measurements. Formation of S_4N_4 also confirmed the role of hexamethyldisilazane as a reductant. Obtained nanoparticles were characterised by PXRD, EDAX, FTIR, FESEM, TEM, HRTEM and UV measurements.

Introduction

Chemical syntheses of nanoparticles (NPs) are attractive because of the ability to manipulate the properties of NPs by simple modification of reagents, capping agents and synthetic conditions. [1-6] To achieve a generalized synthetic approach for any material, a thorough understanding on the nature of intermediate species involved in the synthetic procedure is needed. Even though potential benefits of colloidal synthesis are well explored, [7-12] establishing a generalized procedure for the synthesis of NPs hardly been realized. Reason may be the lack of understanding of chemistry behind the formation of NPs. This situation made colloidal synthesis as a combinatorial play of starting materials and capping agents rather than scientific approach.

Ag_2S is typical functional material with the band gap of 1.1 eV. [13a] Applications like solar cell, [13b] photocatalysis, [13c] water splitting, [13d] nanoprobes, [13e] hydrogen production, [13f] transistors, [13g] bioimaging, [13h] was demonstrated with Ag_2S nanoparticles. Wet chemical synthesis of Ag_2S nanoparticles is preferable because of its tunability and favourable manipulation of required properties. Various synthetic procedures were established to synthesise high quality Ag_2S nanoparticles and made Ag_2S as a competitive functional material among other chalcogenides. [14]

In the present work, Ag_2S NPs were synthesized by hexamethyldisilazane assisted synthetic method. [15, 16] Nano characterizations revealed that Ag_2S NPs were with a bulk crystal structure. While elucidating the reaction pathway of Ag_2S

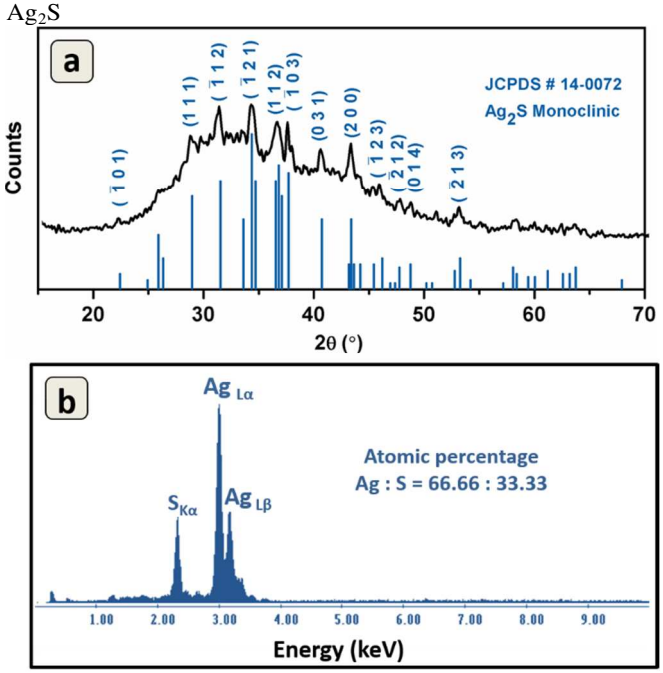

Fig. 1 (a) PXRD pattern of synthesised Ag_2S nanoparticles. Obtained pattern was plotted with standard pattern for visual comparison. Vertical lines represent standard monoclinic Ag_2S diffraction pattern from JCPDS library. Peaks were broadened due to smaller size of nanoparticles. (b) EDAX spectrum of Ag_2S nanoparticles: Peaks are labelled as per energy values. Relative atomic ratio of Ag and S is 2 and 1 respectively. Absence of Silicon signal in spectrum indicates complete removal of capping agent (HMDS).

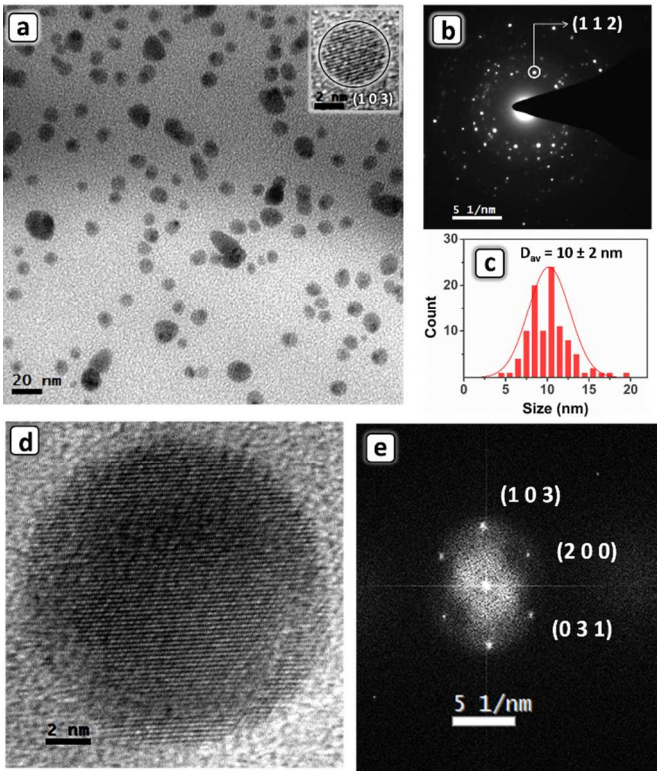

Fig. 2 (a) Representative TEM micrograph of Ag_2S NPs. Inset: HRTEM image of dominant (1 0 3) plane. (b) SAED pattern of the a few NPs. (c) Particles distribution diagram. Particles were ranged from 4 to 19 nm with average diameter of 10 ± 2 nm. (d) High resolution TEM image of single Ag_2S nanocrystal. Clear lattice points confirmed the crystalline nature of NPs. (e) Corresponding FFT image of the nanocrystal.

formation, we have identified Ag NPs and two intermediates viz.; S-N polymer and S_4N_4. The polymeric intermediate was earlier evidenced using GPC (M_w = 2908 and M_n = 2684; PDI = 1.08) and NMR data [15, 16] and further confirmed now by HRMS. Isolated red-orange crystalline S_4N_4 was confirmed by single crystal X-ray diffraction study. The S-N polymer might have decomposed to yield S_4N_4. Isolation and characterization of two intermediates from this reaction concluded the steps involved in the hexamethyldisilazane assisted synthesis of metal sulfides.

Results and Discussion

Ag_2S synthesis

Ag_2S NPs were synthesized using stoichiometric ratio of $AgNO_3$:S = 2:1 in hexamethyldisilazane (Scheme S1, ESI†). Formation of Ag_2S was primarily confirmed by PXRD measurements (Fig. 1a). Obtained patterns were matched with standard bulk phase Ag_2S monoclinic structure (JCPDS # 14-0072). Relative intensities of peaks and positions were matched with standard pattern. The pattern clearly explained the phase purity of Ag_2S and the absence of other stoichiometric ratios. Peaks were broadened and merged with adjacent peaks. This can be attributed to smaller size of synthesised NPs. Contribution of organic moieties for line broadening can be excluded from the absence of HMDS in EDAX spectrum (Fig. 1b). EDAX spectrum confirmed the atomic ratio Ag:S = 2:1 of the samples. Ratio was very uniform throughout the analytical sample. Since there was no signal of oxygen (for $AgNO_3$), silicon (HMDS) or carbonaceous materials, phase purity of Ag_2S NPs was self-evident. Furthermore, non-appearance of silicon in the EDAX spectrum clearly revealed the absence of HMDS (capping agent) on surfaces of the NPs. FTIR spectrum of Ag_2S NPs did not show any signature of amines or organic moieties (Fig. S1, ESI†). This observation clearly explained that the surface of NPs was clean and no capping agent on surfaces.

Microscopic studies

Morphology of Ag_2S NPs determined by scanning electron microscopy (Fig. S2, ESI†) showed spherical nature. Because of the limitation of FESEM resolution, NPs appeared as agglomerated with each other. But particles were well separated as seen in TEM. The particles abundance was high and distribution of particles was ob-served even at micron level. Particle distribution, crystallinity and phase of Ag_2S nanocrystal have been determined by transmission electron microscopy (Fig. 2).

TEM analysis duly confirmed the spherical shapes of NPs (Fig. 2a). NPs were monodispersed and abundant. Particles sizes were ranged from 4 to 19 nm with average size of 10 ± 2 nm (Fig. 2c). Uniformity in size may be attributed to excess availability of hexamethyldisilazane (capping agent) in the reaction. Selected area electron diffraction (SAED) analysis of NPs showed clear dotted pattern (Fig. 2b). This observation clearly revealed the single crystalline nature of obtained NPs. Obtained planes of SAED pattern were matching with PXRD pattern of NPs. For a detailed analysis, a single NP was focused to atomic level and their corresponding two-dimensional fast Fourier transformations (FFT) were obtained (Fig. 2d and 2e). HRTEM analysis of NPs showed interplanar distance of 2.04 Å, which was because of one of the dominant $d_{(1\ 0\ 3)}$ planes of silver (I) sulfide in PXRD pattern. UV-Vis spectra of the nano-particles showed characteristic broad absorption of Ag_2S (Fig. S3, ESI†). [17]

Table 1. Details of controlled reactions performed to establish mechanism

S. No	Reactions	Products
1	$AgNO_3$ + S	No Reaction
2	$AgNO_3$ + HMDS	Ag Nanoparticles
3	S + HMDS	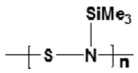
4	2 $AgNO_3$ + S + HMDS	Ag_2S nanoparticles + S_4N_4

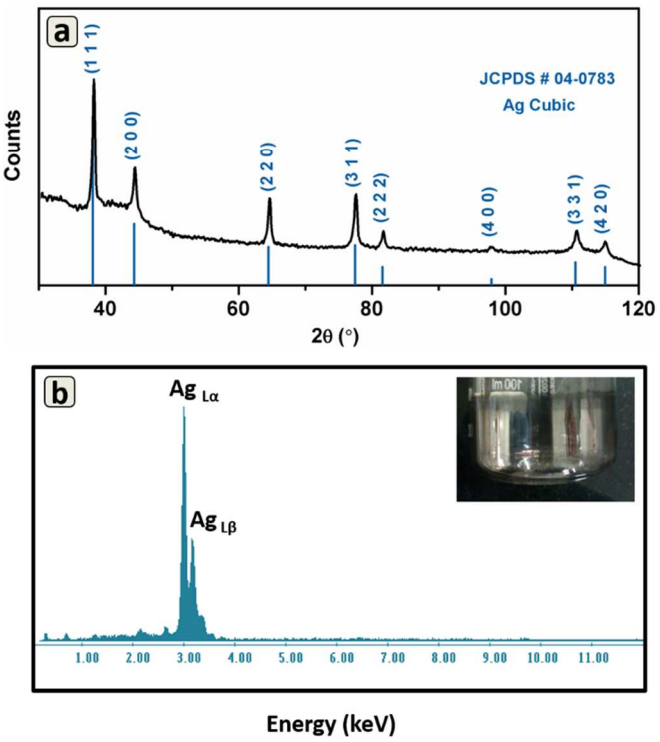

Fig. 3 (a) PXRD pattern of obtained Ag nanoparticles. The pattern was plotted with standard pattern for visual comparison. Vertical lines represent standard cubic Ag diffraction pattern from JCPDS library. (b) EDAX spectrum of Ag nanoparticles. Peaks are labelled as per energy values (Inset: Silver deposition on beaker).

Controlled reactions

In many reactions involving sulfur and nitrogen, in-spite of isolating pure products, the nature of intermediate steps were unclear. In our earlier reports on hexamethyldisilazane assisted syntheses of metal sulfide NPs, isolation of an S-N polymer as intermediate species was described. [15, 16] However, the nature of reduced sulfur was not apparent. To comprehend the reaction pathway of Ag_2S formation, four controlled reactions were conducted (Table 1). While the reaction of $AgNO_3$ with S (reaction 1) did not form any product, the reaction with HMDS (reaction 2) interestingly yielded phase pure Ag NPs. This reaction also explained the twin roles of HMDS as reducing and capping agent. The reaction between HMDS and S yielding smelly S-N polymer (reaction 3) was well established earlier using GPC and ^{29}Si NMR spectral data. [15, 16] In the present study, HRMS clearly showed repeating unit of SNSi (~74.0202) polymer chains (Fig. 5 and S4, ESI†). Since sulfur was soluble in HMDS, it interacted with HMDS yielding an S-N polymer. Though this polymer was formed in the absence of any metal ions, its formation was faster in their presence. [15, 16] This observation indicated a catalysis or facilitation by metal ions for S-N polymer formation.

Ag nanoparticles

Formation of Ag NPs (reaction 2) was primarily confirmed by PXRD measurements (Fig. 3a). Obtained pattern showed bulk phase Ag cubic structure (JCPDS # 04-0783). Peaks relative intensities and positions were matching with standard diffraction pattern. Peaks were broadened due to the smaller size of NPs. Contribution of organic moieties for broadening can be excluded from the absence of HMDS in EDAX spectra. EDAX spectrum confirmed the purity of silver NPs (Fig. 3b). Silver NPs were very small and suitably followed by TEM analysis (Fig. 4a).

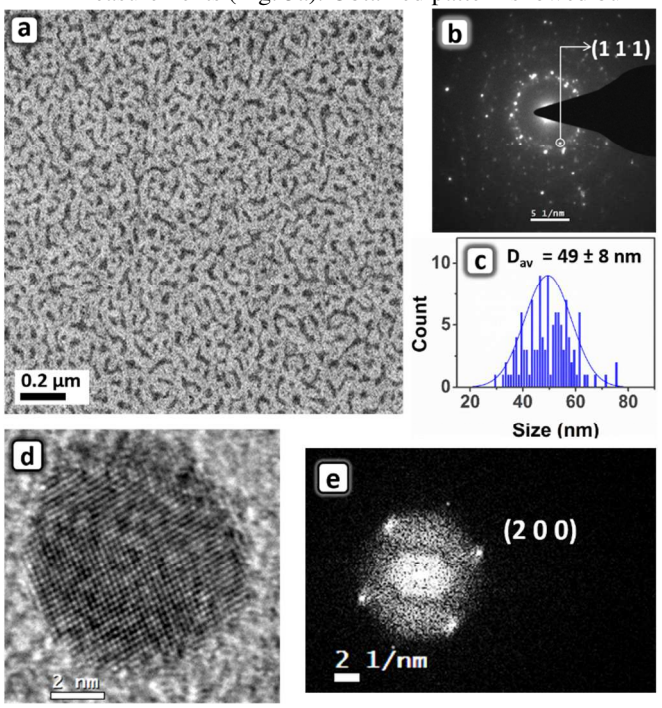

Fig. 4 (a) Large area TEM Micrograph of Ag NPs. (b) SAED pattern of a few NPs and dominant (1 1 1) plane shown. (c) Particles distribution diagram. The particles were smaller and ranged from 29 to 75 nm with average size of 49 ± 8 nm. (d) High resolution TEM image of single Ag nanocrystal. Clear lattice points confirmed crystalline nature of NPs. (e) Corresponding FFT of the nanocrystal and representative (2 0 0) plane were indexed.

TEM images showed the Ag NPs were spherical and abundance was high (Fig. 4a). Since Ag NPs were very small, agglomeration of NPs were observed. Size of NPs ranged from 29 to 75 nm with average size of 49 ± 8 nm (Fig. 4c). Some of the smaller sized nanoparticles also observed in the TEM micrographs. Selected area electron diffraction (SAED) analysis of NPs revealed cluttered spot pattern (Fig. 4b). This may be due to smaller size and wide distribution among NPs. Obtained planes of the SAED pattern were matching with obtained PXRD pattern. To further clarify the orientation, a single NP was focused to atomic level and their corresponding two-dimensional fast Fourier transformations (FFT) were obtained (Fig. 4d and 4e). All Interplanar distances were matched with obtained PXRD pattern. Particles were highly crystalline and no amorphous layer of capping agent was found on the surface. This observation clearly showed complete removal of capping agent on surface of NPs.

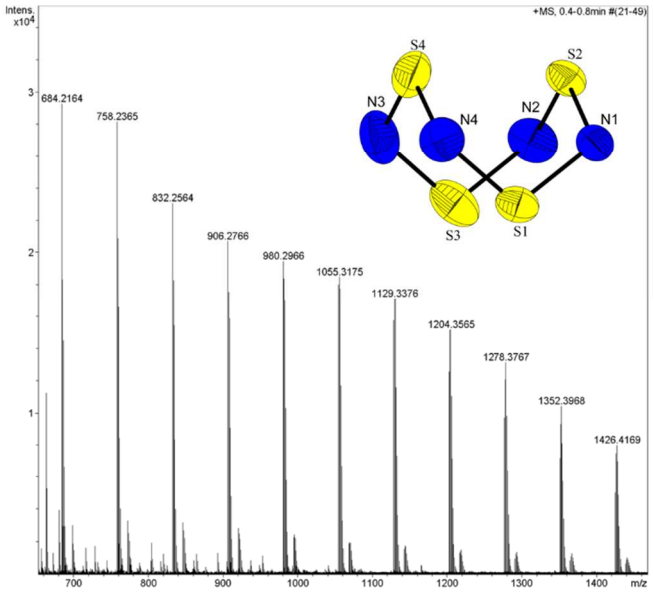

Fig. 5 Isolated intermediates during Ag_2S formation. HRMS data of polymeric intermediate with repeating SNSi unit. Inset: ORTEP diagram of the isolated S_4N_4.

S_4N_4 Isolation

Reaction of stoichiometric amounts of $AgNO_3$ and sulfur in HMDS (reaction 4) led to phase pure Ag_2S NPs formation. From this reaction tetrasulfur tetranitride (S_4N_4) was also isolated (Fig. 5 inset) in a small quantity. S_4N_4 was unambiguously confirmed by single crystal X-ray diffraction analysis of crystals obtained from acetonitrile. The crystal structure (Fig. S5, ESI†) (CCDC 961232) reconfirmed the beautiful cradle structure of S_4N_4. The TGA/DTA analysis (Fig. S6, ESI†) of the crystals showed that it was decomposing at near melting temperature (178.3 °C) reconfirming S_4N_4 formation. S_4N_4 yield was good in higher sulfur ratios ($AgNO_3$:S 2:2) and orange red color in the reaction was very apparent (Fig. S7, ESI†) (Caution: S_4N_4 is an explosive and needs care while varying higher stoichiometry).

Reaction mechanism

Important findings from controlled reactions were no reaction between $AgNO_3$ and sulfur in the absence of HMDS (reaction 1). Reaction 1 revealed that hexamethyldisilazane acted as reducing agent. No S_4N_4 formation was observed in the absence of $AgNO_3$ in the reaction (reaction 3). Hence S_4N_4 not formed by direct reaction between S and HMDS. Reaction 2 clearly explained that S_4N_4 formation was synergistic with Ag_2S formation in HMDS. Controlled reaction conditions also revealed possibility for two parallel reactions *viz.* formation of Ag NPs and formation of Ag_2S NPs. In the absence of sulfur Ag NPs were formed. In the presence of sulfur, phase pure Ag_2S NPs were formed. Moreover no traces of Ag NPs were observed in any kind of analysis along with Ag_2S nanoparticles. Therefore, sulfur reduction and Ag_2S formation in reaction 4 was ensued through three steps. Sulfur was activated by HMDS through S-N polymer formation. The polymer was decomposed to S_4N_4. The worth mentioning here is that S_4N_4 was one of the stable products among smaller S-N cyclic systems [18] and was well known as sulfide source in metal sulfide synthesis. [19] Then the S_4N_4 reacted with Ag^+ ions and promoted the formation of Ag_2S NPs. This can be attributed to the higher activity of sulfide ions towards metallic Ag^+ source.

Conclusions

In summary, complete reaction mechanism of Ag_2S NPs formation was elucidated. Clearly, hexamethyldisilazane assisted synthesis followed a different reaction pathway compared with conventional sulfur-amine "black box" system. [20, 21] Black box systems were explained based on generation of H_2S gas from sulfur-amine system. But in our case, sulfur-amine (hexamethyldisilazane) reaction clearly led to S-N polymer and S_4N_4. Results indicated that present system could be an ideal system for predicting first principles of nanochemistry to establish generalized nanoparticles synthesis.

Experimental Section

All chemicals used in the syntheses were purchased from Aldrich. Standard air-free conditions were maintained throughout the reaction. $AgNO_3$ was chosen for HMDS assisted method for its better solubility and photo stability than silver halides.

Synthesis of Ag_2S nanoparticles

Reaction flask (two-necked round-bottomed flask) containing $AgNO_3$ (0.2 g, 1.18 mmol) and sulfur (0.02 g, 0.62 mmol) was degassed and flushed with dry-deoxygenated N_2. Then HMDS (5 ml, 23.98 mmol; 99.9%, used as received) was introduced into the flask. After purging with nitrogen gas, the reaction mixture was heated to reflux. Even though the formation of Ag_2S was instantaneous, reaction was extended for 1 h for uniform distribution. Black precipitate of Ag_2S was obtained at the end of reaction. Volatile side-products and unreacted HMDS were decanted and residue washed with methanol to remove S_4N_4 traces. Then the black residue was washed with methanol (3×20 ml) followed by toluene (3×20 ml) to remove unreacted $AgNO_3$ and sulfur, respectively. The product was purified under ambient conditions and then dried at 120 °C for 4 h before analysis. The nanoparticles are stable in dark conditions and stored in powder form. S_4N_4 and polymer was isolated from decanted reaction mass. S_4N_4 was extracted from dried filtrate using acetonitrile. Caution: S_4N_4 is an explosive and would explode in dry conditions. S_4N_4 yield was good in higher sulfur ratios (Ag:S 2:2) and isolated comfortably. Polymer was isolated from distilled filtrate.

Synthesis of Ag NPs

Ag nanoparticles were obtained by absence of sulfur source in the reaction. In a reaction flask containing $AgNO_3$ (0.20 g, 1.18 mmol), HMDS (5 ml, 23.98 mmol; 99.9%, used as received) was introduced. After purging with nitrogen gas, the reaction mixture was heated to reflux. The reflux reaction was carried out 24 h for uniform distribution of NPs. Caution: $AgNO_3$ should not be heated without sufficient capping agent. Shiny black precipitate was obtained at end of reaction hours. Volatile side-products and unreacted HMDS were removed under vacuum. The precipitate was continuously washed with methanol (3×20 ml) and shiny silver mirror was obtained at walls of beaker. The product was purified under dark conditions and then dried at 120 °C for 4 h before analysis. Ag NPs were very reactive towards light and transformed to white grey if exposed to light. Most of microscopic analyses were carried out in crude form. All the microscopic measurements were immediately carried out after synthesis to avoid light induced modifications.

Instrumentation

Powder X-ray diffraction measurements were carried out by a Bruker D8 X-ray diffractometer [λ(Cu-K_α) = 1.54 Å] with scan rate of 1° min^{-1}. Powder samples were spread in PMMA holder and the measurements were performed at ambient conditions. Single crystal diffraction measurements were obtained at Oxford CCD X-ray diffractometer (λ = 0.71073 Å). Data reduction was performed using CrysAlisPro 171.33.55 software. [22] The crystal structure was solved and refined using SHELXS-97 and SHELXS-97 respectively. [23] FESEM images of nanoparticles were acquired in Ultra 55 Carl Zeiss instrument operated at variable voltages. The NPs were dispersed in isopropyl alcohol and dry casted on glass/ITO plates. Light exposure was avoided at all occasion while handling samples for microscopic analysis to avoid light induced modifications. TEM micrographs were taken by FEI Technai G^2 20 STEM instrument at an acceleration voltage of 200 kV. The NPs were dispersed in isopropyl alcohol and coated on carbon- coated copper/ Nickel grids (200 mesh). Copper grids were reacted with ionic silver and formed dendrites at edge of all meshes. Hence the nickel grids were utilized for TEM measurements. For all the particle distribution analysis, diameter of 100 particles (randomly) were measured and plotted. IR spectra were recorded with an Alpha FTIR spectrometer. The FTIR spectra were subtracted from the spectrum of pure substrate. TOF and quadrupole mass analyser types were used for HRMS analysis measurements.

Acknowledgements

Authors thank Centre for Nanotechnology for TEM facility and school of physics for FESEM facility both at University of Hyderabad. B.G.K gratefully acknowledges the Council of Scientific and Industrial Research (CSIR), India for Senior Research Fellowship.

Notes and references

School of Chemistry, University of Hyderabad, Hyderabad, India.
E-mail: murali@uohyd.ac.in

Electronic Supplementary Information (ESI) available: FTIR, UV spectrum, HRMS, Single crystal refinement details of S_4N_4 and TGA/ DTA measurements. See DOI: 10.1039/b000000x/

1 (a) Y. G. Sun, Y. N. Xia, *Science*, 2002, **298**, 2176; (b) V. F. Puntes, K. M. Krishnan, A. P. Alivisatos, *Science*, 2001, **291**, 2115; (c) L. Qu, Z. A. Peng, X. Peng, *Nano Lett.*, 2001, **1**, 333; (d) Z. A. Peng, X. Peng, *J. Am. Chem. Soc.*, 2002, **124**, 3343; (e) C. L. Carnes, J. Stipp, K. J. Klabunde, *Langmuir*, 2002, **18**, 1352.

2 (a) J. M. Petroski, T. C. Green, M. A. El-Sayed, *J. Phys. Chem. A*, 2001, **105**, 5542; (b) S. R. Ghanta, K. Muralidharan, *Nanoscale*, 2010, **2**, 976; (c) M. Afzaal, M. Malik, P. O'Brien, *J. Mater. Chem.* 2010, **20**, 4031; (d) W. U. Huynh, J. J. Dittmer, A. P. Alivisatos, *Science*, 2002, **295**, 2425; (e) W. U. Huynh, J. J. Dittmer, W. C. Lippy, G. L. Whiting, A. P. Alivisatos, *Adv. Funct. Mater.*, 2003, **13**, 73; (f) J. S. Steckel, J. P. Zimmer, S. C. Sullivan, N. E. Stott, V. Bulovic, M. G. Bawendi, *Angew. Chem. Int. Ed.*, 2004, **43**, 2154.

3 (a) C. B. Murray, C. R. Kagan, M. G. Bawendi, *Annu. Rev. Mat. Sci.*, 2000, **30**, 545; (b) C. N. R. Rao, A. Govindaraj, S. R. C. Vivekchand, *Annu. Rep. Prog. Chem.*, 2006, **102**, 20; (c) C. N. R. Rao, S. R. C. Vivekchand, K. Biswas, A. Govindaraj, *Dalton Trans.*, 2007, 3728; (d) J. Park, J. Joo, S. G. Kwon, Y. Jang, T. Hyeon, *Angew. Chem. Int. Ed.*, 2007, **46**, 4630; (e) G. M. Whitesides, B. Grzybowski, *Science*, 2002, **295**, 2418; (f) S. Mann, *Chem. Commun.*, 2004, **1**, 1.

4 (a) Z. A. Peng, X. Peng, *J. Am. Chem. Soc.*, 2002, **124**, 3343; (b) C. Burda, X. Chen, R. Narayanan, M. A. El-Sayed, *Chem. Rev.*, 2005, **105**, 1025; (c) Z. Zhuang, Q. Peng, B. Zhang, Y. Li, *J. Am. Chem. Soc.*, 2008, **130**, 10482; (d) M. I. Bodnarchuk, M. V. Kovalenko, W. Heiss, D. V. Talapin, *J. Am. Chem. Soc.*, 2010, **132**, 11967; (e) B. Wiley, Y. Sun, B. Mayers, Y. Xia, *Chem. -Eur. J.*, 2005, **11**, 454.

5 B. L. Cushing, V. L. Kolesnichenko, C. J. O'Connor, *Chem. Rev.*, 2004, **104**, 3893.

6 L. Manna, E. C. Scher, A. P. Alivisatos, *J. Am. Chem. Soc.*, 2000, **122**, 12700.

7 (a) W. Y. Liu, A. Y. Chang, R. D. Schaller, D. V. Talapin, *J. Am. Chem. Soc.*, 2012, **134**, 20258; (b) E. V. Shevchenko, D. V. Talapin, A. L. Rogach, A. Kornowski, M. Haase, H. Weller, *J. Am. Chem. Soc.*, 2002, **124**, 11480; (c) M. Aslam, L. Fu, M. Su, K. Vijayamohanan, V. P. Dravid, *J. Mater. Chem.*, 2004, **14**, 1795; (d) T. K. Sau, C. J. Murphy, *J. Am. Chem. Soc.*, 2004, **126**, 8648.

8 (a) S. Deka, A. Genovese, Y. Zhang, K. Miszta, G. Bertoni, R. Krahne, C. Giannini, L. Manna, *J. Am. Chem. Soc.*, 2010, **132**, 8912; (b) H. Zeng, P. M. Rice, S. X. Wang, S. Sun, *J. Am. Chem. Soc.* 2004, **126**, 11458; (c) S. G. Kwon, T. Hyeon, *Acc. Chem. Res.*, 2008, **41**, 1696; (d) K. K. Caswell, C. M. Bender, C. J. Murphy, *Nano Lett.*, 2003, **3**, 667; (e) Z. S. Pillai, P. V. Kamat, *J. Phys. Chem. B*, 2004, **108**, 945.

9 (a) E. Dilena, D. Dorfs, C. George, K. Miszta, M. Povia, A. Genovese, A. Casu, M. Prato, L. Manna, *J. Mater. Chem.*, 2012, **22**, 25493; (b) D. V. Talapin, J. S. Lee, M. V. Kovalenko, E. V. Shevchenko, *Chem. Rev.*, 2010, **110**, 389; (c) A. Walther, A. H. E. Muller, *Chem. Rev.*, 2013, **113**, 5194; (d) S. V. Kershaw, A. S.

Susha, A. L. Rogach, *Chem. Soc. Rev.*, 2013, **42**, 3033; (e) R. K. Joshi, J. J. Schneider, *Chem. Soc. Rev.*, 2012, **41**, 5285.

10 (a) D. Dorfs, T. Hartling, K. Miszta, N. C. Bigall, M. R. Kim, A. Genovese, A. Falqui, M. Povia, L. Manna, *J. Am. Chem. Soc.*, 2011, **133**, 11175; (b) J. Chun, J. Lee, *Eur. J. Inorg. Chem.*, 2010, 4251; (c) Y. Xia, Y. Xiong, B. Lim, S. E. Skrabalak, *Angew. Chem. Int. Ed.*, 2009, **48**, 60; (d) M. R. Buck, R. E. Schaak, *Angew. Chem. Int. Ed.*, 2013, **52**, 6154.

11 (a) J. Tang, F. Redl, Y. M. Zhu, T. Siegrist, L. E. Brus, M. L. Steigerwald, *Nano Lett.*, 2005, **5**, 543; (b) M. Baghbanzadeh, L. Carbone, P. D. Cozzoli, C. O. Kappe, *Angew. Chem. Int. Ed.*, 2011, **50**, 11312; (c) R. Costi, A. E. Saunders, U. Banin, *Angew. Chem. Int. Ed.*, 2010, **49**, 4878.

12 (a) Z. Q. Yang, K. J. Klabunde, *J. Organomet. Chem.*, 2009, **694**, 1016; (b) F. Li, D. P. Josephson, A. Stein, *Angew. Chem. Int. Ed.*, 2011, **50**, 360; (c) L. Xu, S. Li, Y. Zhang, Y. Zhai, *Nanoscale*, 2012, **4**, 4900; (d) X. Zhang, Q. Zeng, C. Wang, *Nanoscale*, 2013, **5**, 8269; (e) H. Fu, S. W. Tsang, *Nanoscale*, 2012, **4**, 2187.

13 (a) T. G. Schaaff, A. J. Rodinone, *J. Phys. Chem. B*, 2003, **107**, 10416; (b) B. Liu, D. Wang, Y. Zhang, H. Fan, Y. Lin, T. Jiang, T. Xie, *Dalton Trans.*, 2013, **42**, 2232; (c) Y. Xie, S. H. Heo, Y. N. Kim, S. H. Yoo, S. O. Cho, *Nanotechnology*, 2010, **21**, 015703; (d) M. Gholami, M. Qorbani, O. Moradlou, N. Naseric, A. Z. Moshfegh, *RSC Adv.*, 2014, **4**, 7838; (e) Y. Zhang, G. Hong, Y. Zhang, G. Chen, F. Li, H. Dai, Q. Wang, *ACS Nano*, 2012, **6**, 3695; (f) K. Nagasuna, T. Akita, M. Fujishima, H. Tada, *Langmuir*, 2011, **27**, 7294; (g) Z. M. Liao, C. Hou, Q. Zhao, D. S. Wang, Y. D. Li, D. P. Yu, *Small*, 2009, **5**, 2377; (h) X. Zhang, Y. Gu, H. Chen, *J. Innov. Opt. Health Sci.*, 2014, **7**, 1350059.

14 (a) L. Armelao, R. Bertoncello, E. Cattaruzza, S. Gialanella, S. Gross, G. Mattei, P. Mazzoldi, E. Tondello, *J. Mater. Chem.*, 2002, **12**, 2401; (b) M. C. Brelle, J. Z. Zhang, L. Nguyen, R. K. Mehra, *J. Phys. Chem. A*, 1999, **103**, 10194; (c) D. Wang, T. Xie , Q. Peng , Y. Li, *J. Am. Chem. Soc.*, 2008, **130**, 4016; (d) H. Wang, L. Qi, *Adv. Funct. Mater.*, 2008, **18**, 1249; (e) F. Gao, Q. Lu, D. Zhao, *Nano Lett.*, 2003, **3**, 85; (f) A. Sahu, L. Qi, M. S. Kang, D. Deng, D. J. Norris, *J. Am. Chem. Soc.*, 2011, **133**, 6509; (g) J. F. Zhu, Y. J. Zhu, M. G. Ma , L. X. Yang, L. Gao, *J. Phys. Chem. C*, 2007, **111**, 3920; (h) P. Jiang, Z. Q. Tian, C. N. Zhu, Z. L. Zhang, D. W. Pang, *Chem. Mater.*, 2012, **24**, 3; (i) P. Li, Q. Peng, Y. Li, *Chem. -Eur. J*, 2011, **17**, 941; (j) Q. Lu, F. Gao D. Zhao, *Angew. Chem. Int. Ed.*, 2002, **41**, 1932; (k) L. Motte, M. P. Pileni, *J. Phys. Chem. B*, 1998, **102**, 4104; (l) Z. Zhuang, Q. Peng, X. Wang, Y. Li, *Angew. Chem. Int. Ed.*, 2007, **43**, 8174;

15 B. G. Kumar, K. Muralidharan, *J. Mater. Chem.*, 2011, **21**, 11271.

16 B. G. Kumar, K. Muralidharan, *Eur. J. Inorg. Chem.*, 2013, 2102.

17 I. Kryukov, A. L. Stroyuk, N. N. Zinchuk, A. V. Korzhak, S. Y. Kuchmii, *J. Mol. Catal. A: Chem.*, 2004, **221**, 209.

18 T. Chiver, *Acc. Chem. Res.*, 1984, **17**, 166.

19 N. N. Greenwood, A. Earnshaw, Chemistry of Elements, 2nd ed., 1997, p. 725.

20 J. W. Thomson, K. Nagashima, P. M. Macdonald, G. A. Ozin, *J. Am. Chem. Soc.*, 2011, **133**, 5036.

21 (a) S. Mourdikoudis, L. M. L. Marzan, *Chem. Mater.*, 2013, **25**, 1465; (b) R. E. Devis and H. F. Nakshbendi, *J. Am. Chem. Soc.*, 1962, **85**, 543; (c) K. Mori and Y. J. Nakamura, *J. Org. Chem.*, 1971, **36**, 3041; (d) W. G. Hodgson, S. A. Buckler, G. Peters, *J. Am. Chem. Soc.*, 1963, **85**, 543.

22 CrysAlis CCD and CrysAlis RED, versions 1.171.33.55; Oxford Diffraction Ltd, Yarnton, Oxfordshire, UK, 2008

23 G. M. Sheldrick, SHELXS-97, Program for Crystal Structure Solution, University of Gottingen, Gottingen, Germany, 1997.

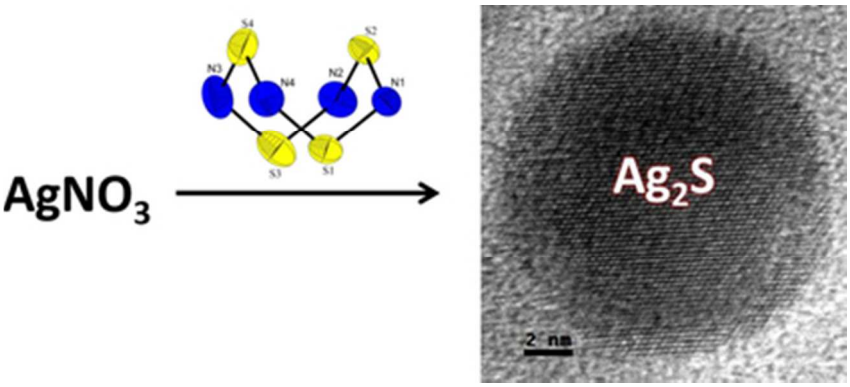

35x15mm (300 x 300 DPI)